Author Accepted Manuscript version of the paper by Øystein Hestad, Torstein Grav Aakre and Lars E. Lundgaard
In IEEE transactions on dielectrics and electrical insulation (2024),
DOI: http://dx.doi.org/10.1109/TDEI.2024.3377178

Conduction and Electric Fields in Dielectric Liquids in Needle-to-Plane Gaps

Øystein L. Hestad, Torstein G. Aakre, and Lars E. Lundgaard

***Abstract*—This paper describes measurements of conduction currents in both neat and commercial insulating liquids. Conduction in thermodynamic equilibrium is measured by applying a low ac voltage in a uniform field. High-field pre-discharge currents are measured in a needle-to-plane configuration stressed with respectively high voltage ac and steep step high voltage pulses. There is a significantly increased conduction for high field compared to low field conditions. Notably, measurements at high fields in needle-plane configurations indicate space charge limitation of currents with polarity differences. The high field conduction exhibits considerable variation across different liquids. At high applied fields, electronic processes are probably governing the charge formation. Simulations indicate that space charges may reduce the local field in front of needle tips at time scales relevant for propagating streamers.**

***Index Terms*—Dielectrics, liquid insulation, mineral oils, esters, cyclohexane, high electric fields, conductivity, space charge limited field (SCLF), space charge limited currents (SCLC).**

I. INTRODUCTION

DIELECTRIC liquids play a crucial role in the insulation systems of various electrical apparatus due to their high electrical withstand voltage and capability as coolants. They find applications in a wide range of apparatus as e.g., transformers, reactors, capacitors, pulse power sources, and X-ray equipment. It is widely recognized that breakdown occurs where the electric field is high, such as around sharp defects at electrodes or at particles in the high field region in the liquid. For ac and impulse voltages, it is assumed that the electric field is distributed capacitively and determined by the permittivity and geometrical configuration of the materials. Conductive properties and space charge phenomena are typically neglected, except in cases of DC stresses where conductive properties dominate the field distribution [1].

The conductivity of a liquid is primarily attributed to ionic drift and diffusion. In a dc stressed uniform gap, an ohmic current behaviour is observed at low voltage stress as seen in Region 1 in Fig. 1. Conduction is then largely influenced by the number of ions and their mobility. At higher voltages (Region 2), ions are depleted due to electrode processes, leading to a non-ohmic behaviour. Furthermore, at even higher voltages (Region 3), dissociation/ionization of molecules occurs, resulting in an increase in current with voltage. When applying a step voltage, time-dependent currents are observed until equilibrium is reached. Both bulk and electrode processes play significant roles in this phenomenon. Whereas design stresses often fall into Region 1, Region 3 is relevant for conditions where streamers leading to breakdown might occur.

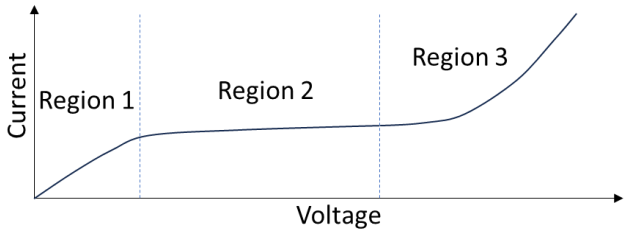

Fig. 1: Sketch of current-voltage characteristics of a dc stressed liquid insulation in a uniform field [2]

Measuring liquid conductivity in an electrode gap with a uniform field becomes challenging at fields exceeding some 10 kV/mm because breakdown then normally occurs caused by field enhancements at irregularities in the electrode surface or by particles [3]. Therefore, conductivity is typically measured at relatively low field stresses. To measure currents at higher electric fields an alternative approach is to use a needle-to-plane electrode configuration. In such a geometry the Laplacian electric fields can reach as high as 1000 kV/mm without causing breakdown, while the total current can be easily measured under dc. However, if using a time-variant ac or stepped voltage there will be both conductive and capacitive currents, where the capacitive component must be subtracted to obtain the conduction currents.

This paper focuses on currents and space charge behavior under high field conditions established in needle-plane gaps, with the aim of understanding conditions relevant for inception and propagation of discharges and streamers. First, we provide a brief review of relevant theories and experiments. Subsequent, we demonstrate the field-dependence of currents under both low-frequency AC and steep-front step voltages in several liquids of both scientific and technical interest. The low voltage and high voltage ac tests refer to previously published results [4], while the main part of the paper with step voltage results are previously unpublished. Finally, we discuss the nature of the high field currents measured, and the implications

This work was supported in part by The Research Council of Norway under contract 294508. The project was also supported by Statnett SF, Statkraft SF, Elvia AS, ABB, Infineon, Equinor, Total and Aker BP. *(Corresponding author: Lars E. Lundgaard).*

Ø.L. Hestad is with SINTEF Energi AS, Trondheim, Norway (e-mail: oystein.hestad@sintef.no).

T.G. Aakre is with SINTEF Energi AS, Trondheim, Norway (e-mail: torstein.aakre@sintef.no).

L.E. Lundgaard is with SINTEF Energi AS, Trondheim, Norway (e-mail: lars.lundgaard@sintef.no).

Color versions of one or more of the figures in this article are available online at http://ieeexplore.ieee.org

Author Accepted Manuscript version of the paper by Øystein Hestad, Torstein Grav Aakre and Lars E. Lundgaard
In IEEE transactions on dielectrics and electrical insulation (2024),
DOI: http://dx.doi.org/10.1109/TDEI.2024.3377178

of these findings for the estimation of the local fields that may occur prior to a streamer initiation and during propagation.

II. Background

This section gives a short overview of some of the most important mechanisms for charge generation and transport in liquids.

A. Bulk effects at low and moderate fields

A dielectric liquid can be considered as a weak electrolyte, where dissociation is the main source of charges. Many of the theories for conduction in liquids therefore relate to electrolytes, being aqueous solutions with a much higher ion density than found in a dielectric insulating liquid [5, 6]. The theories mainly address dc conditions applied in a plane-to-plane uniform gap between metallic electrodes, differentiating between bulk and electrode phenomena and covering conditions from zero to moderate fields [6].

A liquid is at thermodynamic equilibrium at zero and low fields, with a dielectric relaxation time constant of $\tau = \varepsilon/\sigma_0$, where ε is the permittivity and σ_0 is the equilibrium conductivity. The conductivity depends on the number of charge carriers (ions and/or electrons) and their mobilities. For the bulk liquid the measured current will for low fields have an ohmic behavior. When the ion transport time between electrodes approaches the relaxation time, then currents will no longer increase proportional to voltage because ions are swept out of the bulk volume. When further increasing voltage field enhanced dissociation in the bulk will start producing ion pairs, and currents increases again.

There are two standards for measuring conductivity in liquids for electrotechnical use; IEC 61620 applying a low frequency square voltage giving a field below 0.1 kV/mm and IEC 60247 [7, 8] using an ac voltage giving an applied field in the range 0.05-0.25 kV/mm.

B. Electrode effects and space charge limitation

Even without applied voltage there will be a thin double layer of ions at the metallic electrodes depending on the work function of the electrode material. Then, when applying a low voltage, the barrier from the double layer will be disturbed by the weak charge and current injection that takes place. When further increasing the voltage, the charges will be produced faster than bulk currents can transport it away from the electrodes. There will then be a charge build up and the local field will be reduced from these homocharges, which again influence the charge injection. At this point, the currents become space charge limited and increase proportional to the voltage squared [9].

It can be difficult to distinguish bulk and electrode phenomena particularly at higher fields. However, it is experimentally observed that at low field bulk liquid dissociation due to Thomson-Onsager dominates, whereas for higher fields ion injection from the interfaces is the main source for the currents [1].

At increasing voltages, the current carrier density in the high field region increases, and the space charges will limit the field below the Laplacian field, resulting in a space charge limited current. The equation for a plane-plane gap is easily derived from the electrostatic equation $\varepsilon_r\varepsilon_0\frac{dE}{dx} = \rho(x)$:

$$j = \frac{9}{8}\varepsilon\mu\frac{U^2}{d^3} \tag{1}$$

where $\rho(x)$ is the charge density in 1D, j is the current density, $\varepsilon = \varepsilon_r\varepsilon_0$ the permittivity, μ the mobility, U the applied voltage, E the electric field, and d the gap distance.

Similar effects will take place for needle-to-plane gaps and are described by the following equations [10, 11]:

$$I^{0.5} = K(U - U_0) \tag{2}$$

$$K \approx 2.01\left(\frac{\varepsilon\mu}{d}\right)^{0.5} \tag{3}$$

$$U_0 = 0.5E_\mathrm{p}r_\mathrm{p}\ln\left(\frac{4d}{r_\mathrm{p}}\right) \tag{4}$$

where U is applied voltage, U_0 a threshold voltage, ε the permittivity, μ the mobility, d the needle plane gap distance, E_p the needle electric field, and r_p the needle tip radius.

These models are, however, unable to model conditions for very high fields that can be established in needle-to-plane geometries (i.e. > $5{\cdot}10^4$ V/mm). Until better models are established one has to rely on measurements to characterize currents [6].

C. High field phenomena

At high electric fields the conductivity of dielectric materials is typically seen to increase exponentially with the electric field. This conductivity depends on both the charge generation and the mobility of the charge in the dielectric [12]. To calculate the overall current and the effect on the field distribution in the dielectric one needs to understand both how the charge is generated and transported, considering the feedback effect field enhanced charge generation will have on the local fields.

Conduction in bulk liquids is normally associated with ion mobility [13], as electron charges normally are highly localized with short lifetime. However, increasing the electrical fields will lower the barriers towards both drift and generation of electrons. Both the Poole-Frenkel model and the hopping model can account for this. These models have, like the models for injection from electrons, also been elaborated on, including distribution of local traps in the dielectric tunneling between traps, and variable hopping range [14, 15].

For very high electrical fields the injection barrier at the electrode is sufficiently lowered to enable injection of electronic charge directly into the liquid. The two main mechanisms for this are the Schottky injection mechanism (thermionic injection) and the Fowler-Nordheim mechanism (tunnelling thorough the barrier). These models can be further developed to include the effect of localized states close to the electrode (e.g., molecules with low ionization potential (IP) and/or high electron affinity) where electrons or holes can tunnel/jump to at a lower energy cost.

Author Accepted Manuscript version of the paper by Øystein Hestad, Torstein Grav Aakre and Lars E. Lundgaard
In IEEE transactions on dielectrics and electrical insulation (2024),
DOI: http://dx.doi.org/10.1109/TDEI.2024.3377178

III. Experiments

The study comprises three different experiments illustrated in Fig. 2. First, conductivity measurements were done at a low field in a small uniform gap. Next, currents were measured under low frequency ac stress using a needle-to-plane gap. Finally, currents were measured under fast rise step voltage stress in a needle-to-plane gap using a differential electrode set facilitating suppression of the capacitive currents.

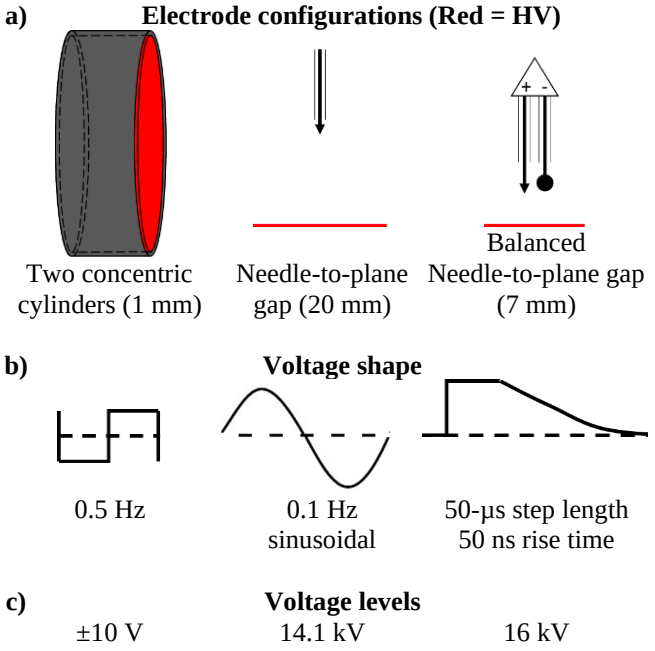

Fig. 2: Overview of electrodes a), voltage shape b), voltage frequency, rise time, and c) max. voltage amplitude. The gaps between high voltage (red) and ground electrode (black) are to scale between the three electrode configurations.

A. Low field conductivity measurement

Experimental set-up and conditions

The low field conductivity and permittivity measurements were carried out at room temperature in accordance with IEC 61620, using the IRLAB LDTRP-2 test equipment. The moisture content of the liquids was determined using a Metrohm 737 coulometer, whereas the density measurements were performed using a Densito 30 PX instrument. The viscosity values were found from the liquids' datasheets.

Results on low field conductivity

Previously published results from the low field measurement are given in TABLE 1 [4]. These conductivities are close to σ_0, representing a system in thermodynamic equilibrium.

TABLE 1:
Low-Field Conductivity and Permittivity Measured According to IEC 61620.

Liquid	Conductivity [pS/m]	Relative Permittivity	Water [µg/g]	Density [kg/m^3]	Viscosity [mm^2/s]
Cyclohexane	1.04	2.01	17	777	1.26
New mineral oil	0.60	2.17	10	872	7.6
Used mineral Oil	22.0	2.23	12	870	-
Synthetic ester	26.6	3.17	200	970	28

B. High field current measurement under AC

Experimental set-up and conditions

These measurements were done using a guarded needle with a tip radius of 5 µm at 20 mm distance from the plane electrode. A 0.1 Hz sinusoidal voltage was supplied from a Trek 20/20C-HS. The applied voltage was 0-30 % below the partial discharge inception voltage. The current measured at the guarded needle was amplified by a current amplifier *SR 570*. A 14-bit high resolution analogue-digital converter and numerical removal of capacitive currents were used to extract the small conductive currents [4].

Results on high field ac conductivity

As voltage was raised, a nonlinear relation between measured current and applied voltage was seen, and for some liquids there was an asymmetry between positive and negative polarity as shown in Fig. 3. Plotting the instantaneous current versus the voltage squared reveals almost linear correlations above a certain voltage threshold.

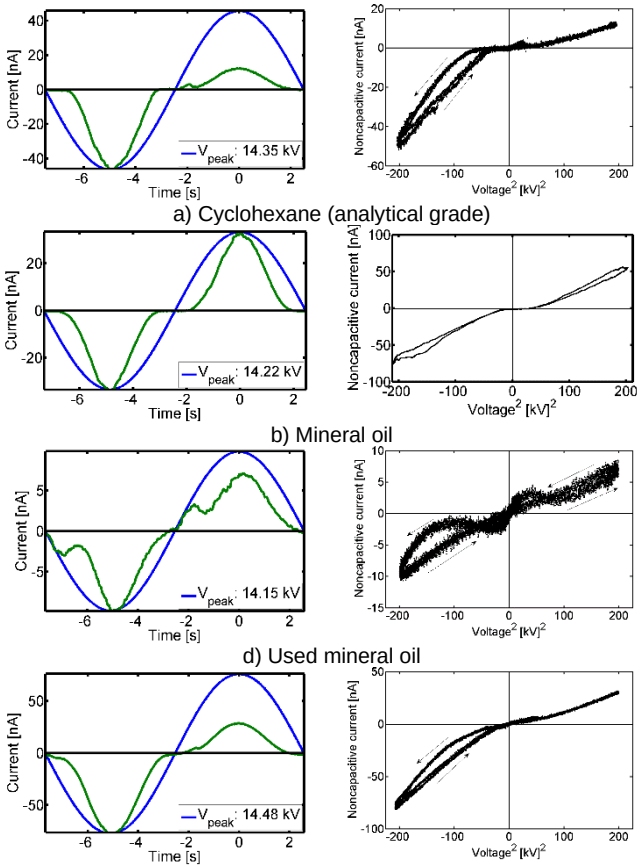

Fig. 3: Measured currents in different liquids at 0.1 Hz sine around 14.3 kV_{pk}. The figures to the left are the current vs phase, the figures to the right are the current vs square of voltage. Graphs from [4] (© [2014] IEEE)

C. High field current measurements under step voltage

Experimental set-up and conditions

A Behlke solid-state switch supplied a step pulse voltage, with typical applied voltage waveforms as shown in Fig. 4. The voltage rise was 50 ns. After a short overshoot the voltage remained constant for 50 µs before decaying with a half-life

Author Accepted Manuscript version of the paper by Øystein Hestad, Torstein Grav Aakre and Lars E. Lundgaard
In IEEE transactions on dielectrics and electrical insulation (2024),
DOI: http://dx.doi.org/10.1109/TDEI.2024.3377178

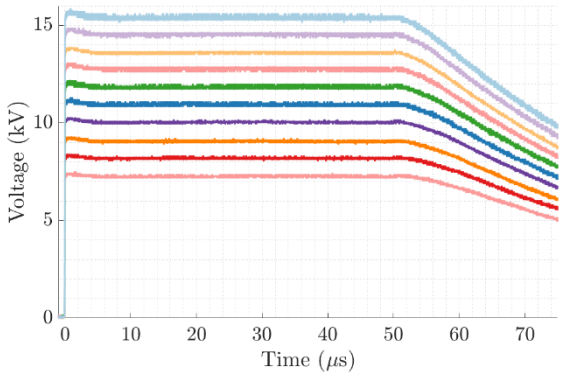

Fig. 4: A typical example of a measured voltage waveforms.

time of 40 µs. At least three voltage impulses were applied at each voltage level to check reproducibility. When approaching streamer inception voltage six step voltages were applied at each voltage level to have a better chance to detect events without streamer occurrence.

The test cell comprises a sharp 3.4 – 4.2 µm radius needle and a spherical probe of about 1 mm diameter over a plane HV-electrode. The needle-to-plane distance was 7 mm, and the probe distance was adjusted with a micrometer screw until its capacitance towards the plane was equal to that of the needle. The needle electrode was made by electrochemical etching of a 100 µm diameter tungsten wire. The same needle was used throughout all measurements. Discharges were avoided as far as possible to reduce erosion of the needle tip. The needle tip radius was measured using a microscope before and after the experiments to ensure that it was not damaged during the experiments. Images of the needle electrode before and after testing are shown in Fig. 5, and the needle was additionally investigated between the tests of the different liquids. The test cell and needle were rinsed before each test with the same liquid type to remove any residues from previous testing.

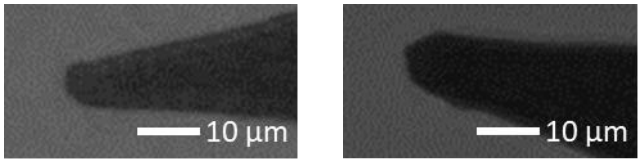

a) Radius before: 3.4 µm b) Radius after: 4.2 µm

Fig. 5: Pictures of the needle electrode before and after the current measurements of all the liquids.

The conduction currents were measured using a differential charge measurement technique as described in [16-18]. The currents at the electrodes were integrated using equally sized capacitors (class 1 ceramic plate capacitors from BC components, 480 pF + cables 50 pF), connected to a high impedance differential amplifier (LeCroy DA 1850A: 1 MHz bandwidth setting). The voltage over the capacitances measured the total charge as a function of time. While the sharp electrode will draw both a capacitive and a conductive current, the probe will only draw a capacitive current. Subtracting the probe charge from the needle charge leaves the charge resulting from the conduction current. Calibration was done by applying a low step voltage and then adjusting the probe distance until the oscilloscope reading was minimized.

The following liquids were chosen in this study: *cyclohexane*, of both analytic and spectroscopic grade as references, unused transformer mineral oil *Nytro 10XN*, and a synthetic ester *Midel 7131* with two different water contents. The cyclohexane was used as-is from new bottles. The transformer oil was first circulated, degassed under vacuum, and filtrated with a 1-µm filter in a large rinsing plant for a long time (days). The dry synthetic ester sample was taken from a barrel, dried and degassed under vacuum for one day. The wet sample was taken directly from the barrel. The water content was then measured.

Results on high field conductivity

The reported integrated charge shown in the following figures refers to the polarity of the high voltage plane electrode. Thus, a *positive* needle will show a *negative* charge. For all figures the same color coding is used for the voltages.

For *spectroscopic grade* cyclohexane linearly increasing charge indicating constant currents were observed for a positive needle as shown Fig. 6. Large streamers >40 pC occurred at 15.4 kV right after voltage application and is indicated as a vertical line at t = 0. For negative needle no pre-inception currents were seen.

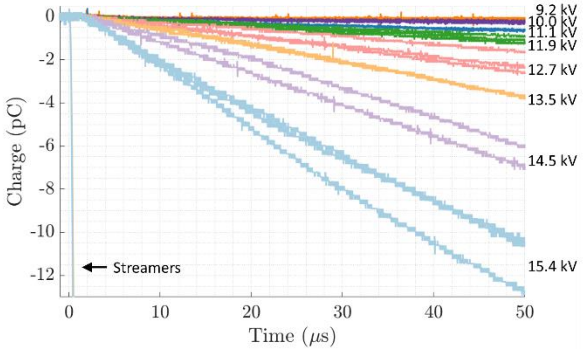

Fig. 6: Integrated currents during positive needle voltage application at indicated voltage levels for spectroscopic grade cyclohexane with needle radius of 4.2 µm.

However, for negative polarity in *analytical grade* cyclohexane a few small pre-inception currents were seen. The onset voltage of measurable pre-inception currents overlapped with the streamer inception voltage, making the observation of pure conductive currents very rare.

For mineral oil, almost linearly increasing charge versus time was seen both for positive and negative voltage steps as shown in Fig. 7. For both polarities the gradient was slightly higher initially than later during the voltage step. Above a certain voltage level, faster initial charge increase or charge steps could be seen. However, after these steps, the charge continued to increase almost linearly like below this threshold.

Zooming in at the initial ten microseconds of the recorded charge in Fig. 8 shows first, faster increase above a certain threshold voltage for both polarities. This can either be slower linearly or faster stepwise increases. After the first fast step, the charge continues to increase linearly like for the lower voltages showing constant currents increasing with increasing voltages.

Author Accepted Manuscript version of the paper by Øystein Hestad, Torstein Grav Aakre and Lars E. Lundgaard
In IEEE transactions on dielectrics and electrical insulation (2024),
DOI: http://dx.doi.org/10.1109/TDEI.2024.3377178

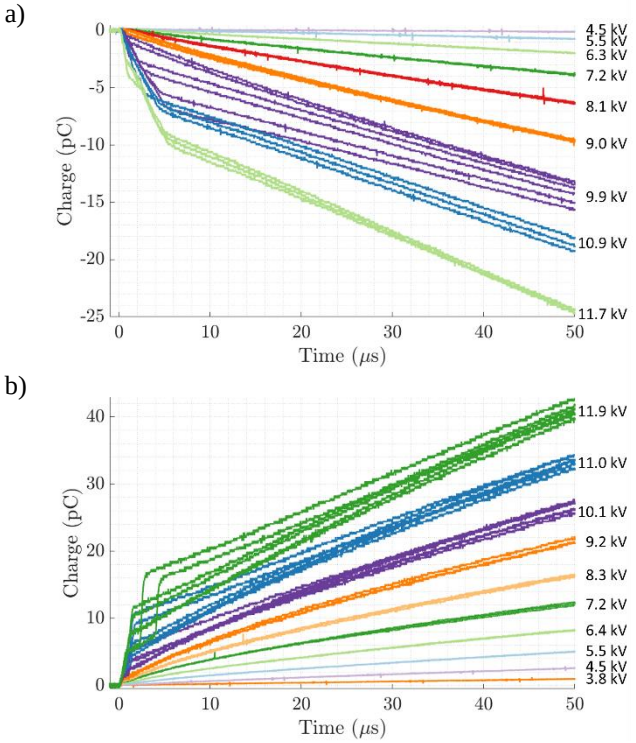

Fig. 7: Integrated currents in mineral oil for a) positive and b) negative needle voltage with 3.4 µm tip radius.

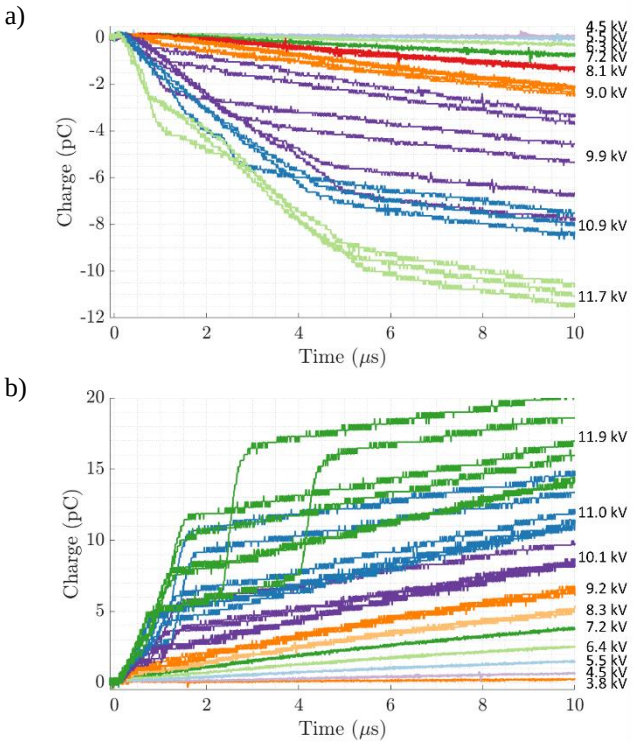

Fig. 8: First part of integrated currents seen in mineral oil for a) positive voltage step and b) negative needle voltage.

Fig. 9 shows the measurements for dry ester. As seen for positive needle no steps were seen except for at high voltages. Then it showed an immediate high charge step probably associated with a streamer inception. This is shown by the light blue curves in Fig. 9 for the two steps at 15.4 kV. Small fast-rising steps can be seen for negative needle polarity at 10 kV. For the wet ester these steps became larger and more frequent.

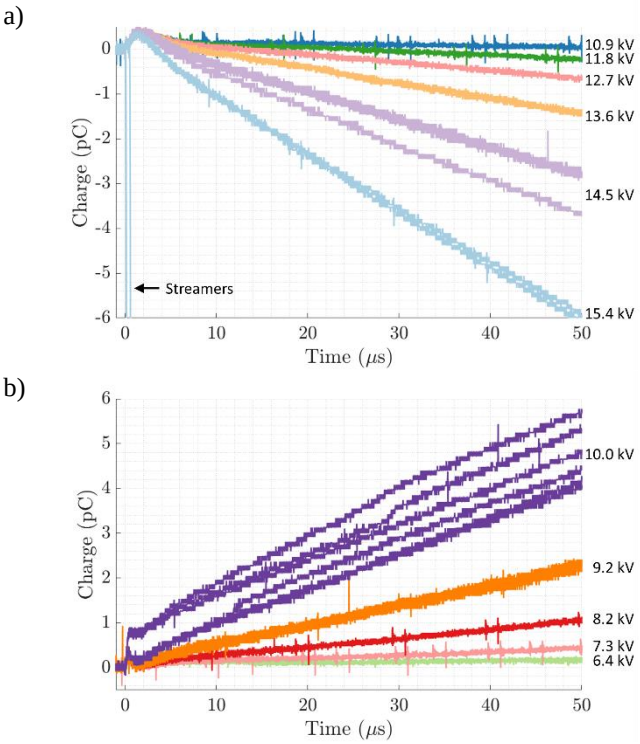

Fig. 9: Integrated currents seen in dry ester for a) positive and b) negative needle voltage with 3.7 µm needle. The first step (2 µs) is probably caused by very small capacitive differences, not possible to equalize.

Currents can be found by taking the average gradient of the charge increase from Figs 6-9. Fig. 10 gives an overview of all the calculated average currents when applying a step voltage. For all curves not showing an initial step, the currents are plotted by the colored data points. Then, for all liquids and

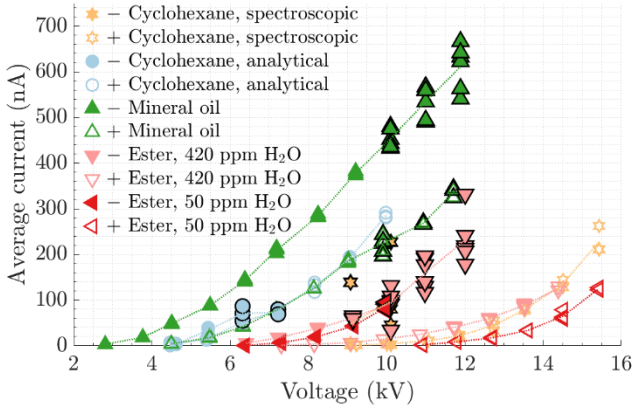

Fig. 10: Current versus voltage for the different liquids at positive and negative stepped voltage. Currents were calculated from the even charge increase seen from the current integration between 10 µs and 50 µs after the voltage step. Black marker edges indicate that a current step occurred during the first 10 µs.

polarities that showed an initial step, currents were derived using the charge increase in the interval between 10 and 50 µs. This is shown by the black marker edge on the data points in Fig. 10. The figure shows that except for the steps, there is a monotonous increase of current with voltage. All datapoints represent a charge measurement above noise level.

IV. Discussions

Conduction currents have been measured for different geometries and voltage shapes in a range of dielectric liquids. The currents measured under AC conditions can be used to make rough approximations of conductivity and mobility, and these can be compared with what would be expected using low-field conductivities. For the currents measured under impulse conditions, we will propose tentative models invoking electronic processes that may explain the results from our measurements. In the following discussion, we will address the validity of employing low-field conductivity for field calculations in conditions close to streamer initiation. Often, Laplacian conditions, which are free from space charges, are assumed when calculating electric fields for discharges and streamer initiation.

A. AC Experiments

The voltages applied during AC current measurements were just below the onset of discharges. Above a certain threshold voltage, the currents increased more or less proportionally with the square of the voltage as seen from Fig. 3, indicating the presence of space charge limitation. Several of the liquids showed higher currents during the negative half cycle of the ac voltage than during the positive half cycle. This suggests the existence of a polarity-dependent charge injection mechanism from the electrode. If all space charges were formed in the bulk liquid by dissociation one would not have seen any polarity dependence. The electric field is not varying much close to the needle when a stable space charge limited field is established, meaning that homocharge and heterocharge have the same field when travelling for a distance. The difference in charge injection may be explained by a lower barrier for the injection of electrons compared to injection of holes.

Assuming a uniform current distribution across a thin liquid layer at the hemispherical end of the tip having an area of 157 µm² (equivalent to the area of a half-sphere with a diameter of 5 µm) and a low field conductivity of 1 pS/m, as measured for analytical cyclohexane (refer to TABLE 1), the electric field can be calculated using the following relationship: $j = I/A = \sigma \cdot E$. The peak current during the negative half cycle was 40 nA (Fig. 3a). Thus, the field strength is calculated to be $2.55 \cdot 10^8$ kV/mm, a value that clearly exceeds any physically meaningful magnitude. This suggests presence of homocharge in the vicinity of the tip, which will limit the electric field and also increase the conductivity of the liquid. The reduction on the field can be approximated by a transition to Space Charge Limited Current (SCLC), seen in Fig. 3a (right) to occur at approximately 7.8 kV for negative currents. This corresponds to an electric field of approximately 830 kV/mm, based on (4). This value is the same order of magnitude as what is typically observed for the Space Charge Limited Field (SCLF) under transient conditions [19, 20]. Assuming that the field is constrained to this value (E_{SCLF}), we can estimate the conductivity at the tip at the voltage peak as follows:

$$\sigma = \frac{I}{A \cdot E_{SCLF}} = \frac{40 \cdot 10^{-9}}{157 \cdot 10^{-12} \cdot 830 \cdot 10^{6}} = 307 \text{ nS/m}.$$

This suggests that the conductivity is approximately 100,000 times higher than what was found for low-field conditions. However, a conductivity of 307 nS/m is still below what is typically expected as the field approaches the Space Charge Limited Field (SCLF) [19, 20]. Here one should consider that at ac voltage, there will be space charges from preceding half cycles, that complicating further analysis.

The curves in Fig. 3 for used transformer oil were different from the others. At low voltage these curves indicate ohmic conduction while at higher voltage the currents seemed to saturate whereafter at even higher voltage the behavior resembles what was seen for the other liquids.

Even though the experiments do not provide conclusive evidence regarding the nature of charge formation, the observed asymmetry, where the negative needle yields higher currents than the positive, suggests the presence of a surface-governed charge injection mechanism.

B. Impulse Experiments

The general picture from the charge measurement in Figs 6-9 shows a constant rate charge increase during the voltage step indicating constant currents. This was seen both for the curves where the charge increase was constant from the time of voltage application and also seen for the cases at increased voltage after an initial step or fast rise charge increase could be seen. Like observed for sinusoidal voltages, negative polarity currents were higher than positive polarity currents. Fig. 10 shows large differences between liquids, from mineral oil having the highest currents to ester and cyclohexane where voltages were much higher before any detectable currents could be measured. For cyclohexane and ester, it was found that the cleaner the liquids, the smaller the currents were. Spectroscopic grade cyclohexane had smaller currents than analytic grade and increasing water content in the ester also increased measured currents.

The initial fast rise charge (high current) seen for positive needle in transformer oil at increased voltages was not seen for cyclohexane and esters. It is unlikely that this first high current stems from streamer initiation. For positive polarity, the critical radius for second mode filamentary streamers is expected to be lower than the tip radius used in these experiments, so any positive streamers should have been of filamentary second mode with a short current pulse, not of microsecond duration as the current rises in Fig. 8 indicate. However, for negative polarity high initial currents were also observed in esters like what was seen for mineral oil.

In general, the current-voltage relation neither fitted linear nor logarithmic correlations. However, as seen from Fig. 11, plotting the square root of the observed currents shows linear relationships starting at various voltage offsets. This has also been reported previously for similar measurements performed in cyclohexane [16].

Author Accepted Manuscript version of the paper by Øystein Hestad, Torstein Grav Aakre and Lars E. Lundgaard
In IEEE transactions on dielectrics and electrical insulation (2024),
DOI: http://dx.doi.org/10.1109/TDEI.2024.3377178

Suggested model for charge generation and drift in high field region

At first glance, all plots (Figs. 6-9) indicate a constant rise of charge, implying a constant current. The same constant rate of charge is seen after a fast rate or stepped charge increase had occurred at the very beginning of the step. In all cases, the current afterward appears to be constant, suggesting an initial high-rate generation of charge carriers followed by drift. However, these initial charge steps were not seen for wet ester and spectroscopic grade cyclohexane under positive polarity.

The measured currents exhibit distinct bulk-limited behavior, characterized by a threshold below which no current is observed and above which the square root of the current is proportional to the voltage as shown in Fig. 11. To explain this behavior, one must consider both charge generation/injection in the high-field region and subsequent charge drift in the volume further away from the tip.

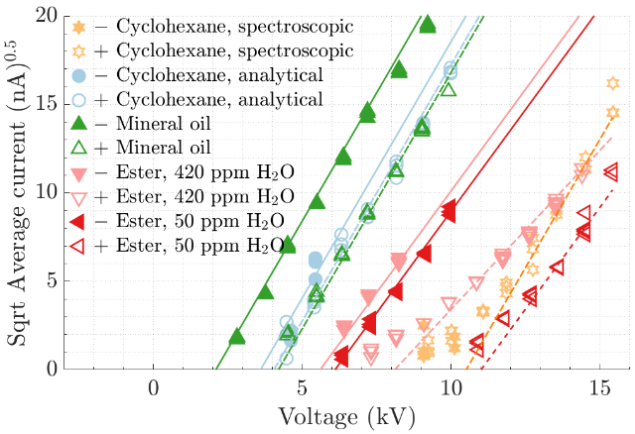

Fig. 11: The square root of the average current measured in the liquids versus voltage. Linear dependence in this plot indicates a SCLC regime

Traditionally, as described in the background section, space charge limited currents in liquids are explained by ionic charge injection from the electrode, restricted by the injected homocharge [13]. The straight lines with square root of current increasing proportional to the voltage plotted in Fig. 11 as described by (2) is indicative of space-charge limitation. The initial local field-governed charge formation is quickly reduced from the injected charges, limiting the local field until an equilibrium between charge injection and charge transport through the liquid is achieved. This model was developed for dc and uniform field conditions [21]. In the transient case presented here with a fifty nanosecond rise time and fifty micro-second step duration, an equilibrium state will not occur. However, under divergent field conditions, a close-to steady state can occur locally in the high-field region when injected charge reduces the field to a level where charge generation/injection ceases. The current is then governed and limited by the mobility of the charge carriers outside the high-field region. Consequently, it is not the charge generation in the high-field region that governs the resulting current. This explains the linear increase in charge with time (indicating nearly constant current) after what appears to be a higher current in the initial microseconds seen in Fig. 7. The initial higher current is likely due to the high field initial charge generation or injection, which quickly lowers the field in the high-field region at or close to the needle.

It is noteworthy that, except for humid ester and spectroscopic grade cyclohexane, the slopes in Fig. 11 are the same both for positive and for negative polarity. The overall trend of the current suggests that it is limited by the mobility of charge carriers in the bulk liquid subsequent to an initial onset of charge generation. Charge mobilities for the liquids for both sinusoidal and step voltages are calculated according to (2) and (3) and shown in TABLE 2. The mobility of cyclohexane is comparable to what has been found before ($3.3{\cdot}10^{-7}$m^{2}V^{-1}s^{-1} [16]).

It can be seen in Fig. 10 that analytical cyclohexane showed a much higher current than spectroscopic grade cyclohexane, while the charge mobilities in the bulk (i.e. blue region in Fig. 12) seems to be similar. The difference between the cyclohexane liquids is their purity. The spectroscopic grade is purer than 99.9 %, and analytic grade purer than 99.5 %. As the mobility is the same for the two liquids, this suggests that the unknown 0.4 % does not change the dominant charge carriers in the liquids. However, as seen from Fig. 11 the purer cyclohexane has a much higher threshold for space charge limited current. This suggests that "contaminates" in the less pure liquid is responsible for the enhanced charge formation at or in the vicinity of the sharp electrode. Similar differences in threshold for SCLC were seen between dry and wet ester at positive polarity, explained by the effect the water has on dissociation in the bulk. However, for negative polarity the effect is small, which would be in line with a surface effect being dominating for negative polarity.

TABLE 2:

CALCULATED MOBILITY FOR INVESTIGATED LIQUIDS UNDER SINUSOIDAL AND STEP VOLTAGE APPLICATION IN A NEEDLE-TO-PLANE GAP IN ACCORDANCE WITH EQUATIONS (2) AND (3).

	STEP, 3.5 µm		**SINE, 5 µm**	
Mobility [$\mathbf{m^2V^{-1}s^{-1}}$]	μ+	μ-	μ+	μ-
Cyclohexane, analytic	$8.2{\cdot}10^{-7}$	$8.2{\cdot}10^{-7}$	$2.8{\cdot}10^{-8}$	$3.2{\cdot}10^{-7}$
Cyclohexane, spectroscopic	$8.2{\cdot}10^{-7}$	N/A	-	-
Mineral oil	$7.6{\cdot}10^{-7}$	$7.6{\cdot}10^{-7}$	$1.4{\cdot}10^{-7}$	$1.3{\cdot}10^{-7}$
Synthetic ester + 50 ppm water	$3.3{\cdot}10^{-7}$	$3.3{\cdot}10^{-7}$	-	-
Synthetic ester + 200 ppm water	-	-	$5.8{\cdot}10^{-8}$	$2.9{\cdot}10^{-7}$
Synthetic ester + 420 ppm water	$2.0{\cdot}10^{-7}$	$3.3{\cdot}10^{-7}$	-	-

The measurements clearly demonstrate the existence of a threshold field for the onset of space charge limited current. This threshold is likely to be linked to charge generation or charge injection at the needle's surface or in its close vicinity. For semiconductors such thresholds are explained by trap depths for either electrons or holes where higher thresholds indicate deeper traps. This fits with ionization potential of aromatic molecules in the mineral oil being lower than in neat cyclohexane.

Author Accepted Manuscript version of the paper by Øystein Hestad, Torstein Grav Aakre and Lars E. Lundgaard
In IEEE transactions on dielectrics and electrical insulation (2024),
DOI: http://dx.doi.org/10.1109/TDEI.2024.3377178

The calculated mobility for the sinusoidal voltage is lower than for the step voltage, differing by about one order of magnitude. Under ac there is a slow formation of local charge during a long sequence, whereas for step voltage this charge formation that is counterbalanced by the charge drift is established momentarily. This altogether suggests a difference in conduction mechanisms where ions dominate for sinusoidal voltage and electrons possibly playing a more critical role for step voltage. Even if macroscopic fields are below what is expected for electronic processes, the local fields at a molecular level can be much higher. Density functional theory calculations including a background field have confirmed that the ionization potential of molecules is lowered like predicted by the classical Poole Frenkel theory, but further shows that the exact relation to the field also depends on the orientation of the molecules in the electric field [22, 23]. In addition, calculation of local fields at molecules depends on the distribution and orientation of nearby molecules and may be order of magnitudes higher than the macroscopic fields [24]. Thus, even in fields where classical theory would imply that no charge generation in the bulk for a neat dielectric with a high ionization potential should be possible, local effects can still lead to charge generation at relatively modest fields.

While these simplified hypotheses of charge formation and charge drift in the high-field region can explain the overall results, uncertainties remain regarding the precise mechanisms of charge formation, dominating charge carriers, and temporal evolution of local fields.

Simplified modelling of high field region conductivity

To gain further insight into how this charge formation may influence the local electric field, simplified numerical simulations were made. The near linear increase in the charge on the needle above the threshold voltage can be explained by an increase in the conductivity that on one hand allows the charge being created in a high field region/injected to move into the liquid, but on the other hand restrict the transport of charge out of this region thus resulting in an accumulation of homocharge that limits the field in the region where charges are formed. Once the field exceeds the threshold field for charge generation, local charge generation increases rapidly. However, outside this region conductivity remains low. This is sketched in Fig. 12.

The simulations were done in COMSOL Multiphysics and based on the following basic electrostatic equations and a field dependent conductivity:

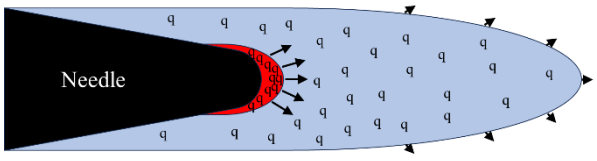

Fig. 12: Sketch of charge generation and transport. Charges are generated in the region with highest field (red). These charges will drift into a low(er) field region (light blue) and a combination of enhanced mobility and charge carrier density will increase the conductivity in this region.

$$\nabla \cdot \boldsymbol{J} = Q_{j,v} \tag{5}$$

$$\boldsymbol{J} = \sigma(|\boldsymbol{E}|)\boldsymbol{E} + \frac{\partial \boldsymbol{D}}{\partial t} + \boldsymbol{J}_e \tag{6}$$

$$\boldsymbol{E} = -\nabla V \tag{7}$$

where $\boldsymbol{J}$ is the current density, $Q_{j,v}$ the free charge, σ the conductivity, $\boldsymbol{E}$ the electric field, $\boldsymbol{D}$ the displacement field, and V the voltage. The resulting apparent conductivity explained in the sketch in Fig. 12 was here approximated to $\sigma(E) = A \cdot \exp\left(B \cdot \sqrt{E}\right)$. A parameter sweep of the constants A and B were performed to find the best fit to the experimental data. For mineral oil the overall trend of the currents can be described by a formula with exponentially increasing conductivity using SI units:

$$\sigma(E) = 5.8 \cdot 10^{-10} \exp\left(5 \cdot 10^{-4}\sqrt{E}\right) \tag{8}$$

The square root dependence is typical for Poole-Frenkel conduction and Schottky injection, but the actual fitted parameters are not in accordance with these mechanisms.

The simulated geometry was rotational symmetric around the center axis with a tip radius of 3.5 µm, a 7-mm gap, and 20 mm radius of liquid making the outer limit. The Mesh was "extremely fine" around the 0.1 mm from the needle tip, and "fine" elsewhere. The applied voltage was mimicking a streamer time scale with a rise time of 1 ns.

The best parameter fit for responses of selected voltages for mineral oil is shown in Fig. 13. While such approaches can reproduce the average currents quite well, they predict a sharper increase in the initial currents, which were only seen experimentally here for the higher voltages in mineral oil. This means that the model includes less current limitation than the measured values. The deviation between modelled and measured current simply shows that the presented conductivity is just an estimate.

Whereas the overall trend of the accumulated charge as a function of time can be reproduced, information regarding the creation and drift of charge in the high field region is limited. This is due to the limitations of the approach taken where simplified conductivity formulas were used to cover both charge generation and drift. In the future an approach where the charge transport equations are solved should be used, as this

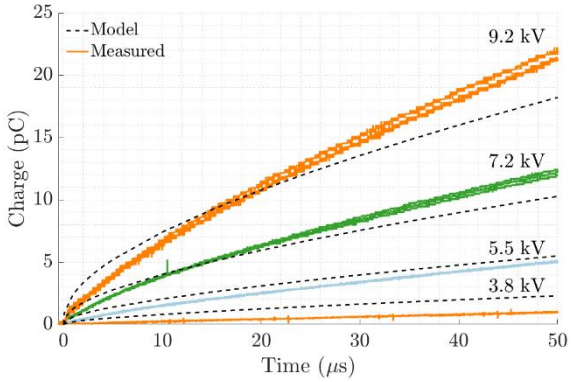

Fig. 13: Measured and simulated accumulated charge as a function of time during the negative step voltage application for mineral oil.

Author Accepted Manuscript version of the paper by Øystein Hestad, Torstein Grav Aakre and Lars E. Lundgaard
In IEEE transactions on dielectrics and electrical insulation (2024),
DOI: http://dx.doi.org/10.1109/TDEI.2024.3377178

will allow to separate between charge generation/number of charge carriers and the mobility of the charge carriers.

In general, the use of a generalized conductivity formula, like (8), to explain both charge generation and charge mobility is not useful, as it was unable to reproduce results for the liquids with high onset fields/voltages for the recorded currents (all liquids except mineral oil). For these the best overall fit to the experimental results were found using a step function in the conductivity "turning on" the conductivity above a certain limit. While such simplified approaches have been used in the past for dielectrics to explain their field dependent behavior, they typically have been used in cases where the conductivity goes from very low to effectively conducting [25]. In the liquids tested using this approach the overall increase in conductivity above the threshold is significant, but not like predicted by the mobility edge theory on which the classical SCLF theory is based [25]. While these conductivity formulas do reproduce the overall current recorded, and the shape of the charge measurements, they predict a constant (and relatively low) conductivity throughout large parts of the dielectric, whereas information regarding the high field region and the effect of charge generation in this region is lost. Thus, limited information can be gained regarding the charge formation and field magnitude in the high field region.

However, one important recognition can be made regarding the spatial extension of the high field region. Any larger regions quickly going from low to high conductivities would result in a marked non-linear increase in the recorded charge on the needle during the first period of the pulse. Whereas such a behavior is observed for mineral oil, the liquids with high threshold U_0 for SCLC we see that the charge injection is nearly linear from the start. This indicates that the charge is generated in a very small region at or outside the needle surface for these liquids.

C. Electrical Field close to the Needle Electrode

While accurately modelling the measured currents remains challenging, it is possible to derive the effect on the local field near the needle tip based on the threshold voltage of the measured currents. Below this threshold, the electrical field distribution will be nearly Laplacian, whereas above it, the field will be constrained by charge formation, and drift in the high-field region. As a first approximation, the electric field on the needle can be estimated by examining the onset field for the Space Charge Limited Current (SCLC) regime, which ranges from 315 kV/mm (mineral oil) up to 1630 kV/mm (ester) for the liquids presented in this paper. While this simplified approach shows the large difference between the liquids, it does not show the time dependence or spatial variance of the field in the liquid. For this a more rigorous numerical approach is needed.

For mineral oil we can use the empirical formula (8) to investigate how the field around the tip will develop above the threshold for SCLC. The electric field in the gap in the vicinity of the needle at increasing time is calculated and shown in Fig. 14. It is seen that the Laplacian field is not valid, even for the first nanoseconds. It is evident from the provided data and the estimation of local fields shown in Fig. 14 that space charges may screen the tip area even during fast transients. This shows that pre-breakdown streamers in mineral oil with sharp-

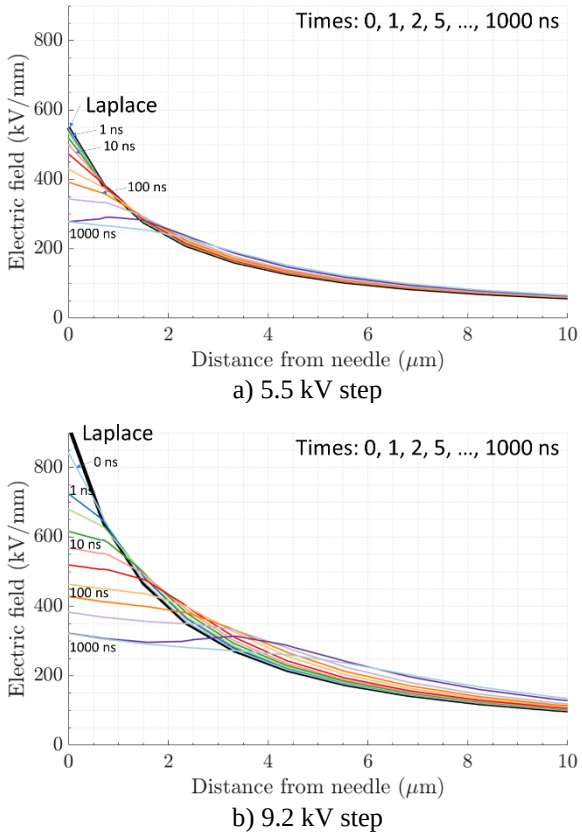

Fig. 14: The estimated electric field in mineral oil close to the negative needle electrode for two voltage amplitudes. Model voltage rise time of 1 ns. The chosen voltages correspond to two measured voltage steps.

ended fast-propagating plasma-filled conducting channels are formed at a lower field than what is predicted by the Laplacian field. Since the generation and distribution of this space charge occurs on similar timescales as a propagating second mode streamer (with a velocity of a few mm/µs), space charges are likely to play a significant role in the propagation phase of a streamer. The wide voltage range within which the speed of second mode streamers for mineral oils is observed to be constant [26] may be explained by a stabilizing effect from high injection currents that limits the local field. Contrary to this, for esters and for cyclohexane, where space charge injection occurs at higher fields, no such stabilization of streamer velocity is seen. For esters, streamers switch from slow second to fast fourth mode propagation without any stabilized interval. Without the stabilizing effect from charge formation, the local fields will be higher and able to support faster propagation as earlier suggested [27].

V. Conclusions

The low field conductivity of dielectric liquids does not reflect conductive phenomena occurring at high fields.

Currents measured for needle-to-plane electrode gaps both for sinusoidal and step voltage stresses appear to be space-charge limited.

Pre-inception conduction currents at step voltage application vary a lot between different liquids.

Calculated mobilities appear lower for sinusoidal than for step voltage stress. Polarity differences in currents and mobilities suggest different charge formation phenomena at electrodes for respectively positive and negative polarities.

Charge mobilities are order of magnitude higher for fast step voltage application than for sinusoidal voltages suggesting electronic effects to take place.

The much higher pre-inception currents seen for mineral oils compared to what is found for synthetic ester and neat cyclohexane will stabilize the field for the mineral oils, and it is suggested that this may explain the different thresholds for faster streamers in the two liquid types.

In general, the use of a generalized conductivity to explain both charge generation and charge mobility fails to reproduce the measured currents for most of the liquids. One exception is the mineral oil with a high measured current at lower voltages.

REFERENCES

[1] U. Gäfvert, A. Jaksts, C. Tornkvist and L. Walfridsson, "Electrical field distribution in transformer oil," in *IEEE Transactions on Electrical Insulation*, vol. 27, no. 3, pp. 647-660, June 1992, doi: 10.1109/14.142730.

[2] A. A. Zaky and R. Hawley, *Conduction and breakdown in mineral oil*. London, UK: Peter Peregrinus, 1973.

[3] A. Küchler *et al.*, "HVDC transformer insulation: oil conductivity," CIGRE technical brochure 646, 2016.

[4] T. Grav and L. E. Lundgaard, "Currents in AC stressed liquid insulated needle plane gap," 2014 IEEE 18th International Conference on Dielectric Liquids (ICDL), Bled, Slovenia, 2014, pp. 1-5, doi: 10.1109/ICDL.2014.6893091.

[5] L. Onsager, "Deviations from Ohm's Law in Weak Electrolytes," *The Journal of Chemical Physics*, vol. 2, no. 9, pp. 599-615, 1934, doi: 10.1063/1.1749541.

[6] A. Denat, "Conduction and breakdown initiation in dielectric liquids," in *IEEE International Conference on Dielectric Liquids*, Trondheim, 2011, doi: 10.1109/ICDL.2011.6015495.

[7] *Insulating liquids - Determination of the dielectric dissipation factor by measurement of the conductance and capacitance*, IEC, 1998.

[8] *Insulating Liquids - Measurement of relative permitivity. dielectric dissipation factor (tan D) and d.c. resistivity*, 60247, IEC, 2004.

[9] A. Castellanos, "Space Charged Limited Currents in Liquid Dielectrics," in *Electrohydrodynamics*, (International Centre for Mechanical Sciences: Springer, 1998, pp. 174-184.

[10] A. Denat, J. P. Gosse and B. Gosse, "Electrical conduction of purified cyclohexane in a divergent electric field," in *IEEE Transactions on Electrical Insulation*, vol. 23, no. 4, pp. 545-554, Aug. 1988, doi: 10.1109/14.7324.

[11] R. Coelho and J. Debeau, "Properties of the tip-plane configuration," *Journal of Physics D (Applied Physics)*, vol. 4, no. 9, pp. 1266-80, 1971, doi: 10.1088/0022-3727/4/9/305

[12] N. Felici and J. P. Gosse, "Injection d'ions par des électrodes métallique dans les hydrocarbures liquides de résistivitié élevée," *Revue de Physique Appliquée*, vol. 14, p. 629, 1979.

[13] A. Castellanos, "Space Charged Limited Currents in Liquid Dielectrics," in *Electrohydrodynamics*: Springer, 1998.

[14] D. Braun, "Electronic injection and conduction processes in polymer devices," *Journal of Polymer Science B*, vol. 41, pp. 2622-2629, 2003, doi: 10.1002/polb.10654.

[15] H. J. Wintle, "Charge motion in technical insulators: facts, fancies and simulations," in *IEEE Transactions on Dielectrics and Electrical Insulation*, vol. 10, no. 5, pp. 826-841, Oct. 2003, doi: 10.1109/TDEI.2003.1237332.

[16] L. Dumitrescu, O. Lesaint, N. Bonifaci, A. Denat, and P. Notingher, "Study of streamer inception in cyclohexane with a sensitive charge measurement technique under impulse voltage," *Journal of Electrostatics*, vol. 53, no. 2, pp. 135-146, 2001, doi: 10.1016/S0304-3886(01)00136-X.

[17] Ø. L. Hestad, L. E. Lundgaard, and D. Linhjell, "New experimental system for the study of the effect of temperature and liquid to solid transition on streamers in dielectric liquids: application to cyclohexane," *Dielectrics and Electrical Insulation, IEEE Transactions on*, vol. 17, no. 3, pp. 764-774, 2010, doi: 10.1109/tdei.2010.5492249.

[18] Ø. L. Hestad, T. G. Aakre, H. Bærug and L. Lundgaard, "Field Dependent Currents in n-Tridecane," *2022 IEEE 21st International Conference on Dielectric Liquids (ICDL)*, Sevilla, Spain, 2022, pp. 1-4, doi: 10.1109/ICDL49583.2022.9830926.

[19] Ø. L. Hestad, P.-O. Åstrand, and L. E. Lundgaard, "N-tridecane as a model system for polyethylene: comparison of pre-breakdown phenomena in liquid and solid phase stressed by a fast transient," *IEEE Transactions on Dielectrics and Electrical Insulation*, vol. 18, no. 6, pp. 1929-1946, 2011, doi: 10.1109/tdei.2011.6118631.

[20] S. Boggs, "Very high field phenomena in dielectrics," *IEEE Transactions on Dielectrics and Electrical Insulation*, vol. 12, no. 5, pp. 929-938, 2005, doi: 10.1109/tdei.2005.1522187.

[21] N. F. Mott and R. W. Gurney, *Electronic Processes in Ionic Crystals*. New York City: Oxford University Press, 1940.

[22] H. S. Smalø, Ø. L. Hestad, S. Ingebrigtsen, and P.-O. Åstrand, "Field dependence on the molecular ionization potential and excitation energies compared to conductivity models for insulation materials at high electric fields," *Journal of Applied Physics*, vol. 109, no. 7, 2011, Art no. 073306, doi: doi:10.1063/1.3562139

[23] N. Davari, P. O. Åstrand, and T. Van Voorhis, "Field-dependent ionisation potential by constrained density functional theory (vol 111, pg 1456, 2013)," *Molecular Physics*, vol. 111, no. 21, pp. 3334-3334, Nov 2013, doi: 10.1080/00268976.2013.836792.

[24] N. Davari, C. D. Daub, P.-O. Åstrand, and M. Unge, "Local Field Factors and Dielectric Properties of Liquid Benzene," *Journal of Physical Chemistry B*, vol. 119, no. 35, pp. 11839-11845, Sep 2015, doi: 10.1021/acs.jpcb.5b07043.

[25] T. Hibma and H. R. Zeller, "Direct measurement of space-charge injection from a needle electrode into dielectrics," *Journal of Applied Physics*, vol. 59, no. 5, pp. 1614-1620, 1986, doi: 10.1063/1.336473.

[26] L. E. Lundgaard, Q. Liu, O. Lesaint and I. Madshaven, "Dielectric Performance of Transformer Liquids–Summary of a CIGRE Study," in *IEEE Electrical Insulation Magazine*, vol. 39, no. 5, pp. 7-16, September/October 2023, doi: 10.1109/MEI.2023.10220158.

[27] L. E. Lundgaard, D. Linhjell, Ø. L. Hestad, M. Unge, and O. Hjortstam, "Pre-breakdown phenomena in hydrocarbon liquids in a point-plane gap under step voltage. Part 2: Behaviour under negative polarity and comparison with positive polarity," *Journal of Physics Communications*, 2020, Art no. 045011, doi: 10.1088/2399-6528/ab7b32.